



The Effect of Dew Point Control on Hydrogen Embrittlement of Al-Si Coated Hot-Stamping Components

H. Z. Lu¹(✉), A. M. Guo¹, Y. Feng², M. T. Ma², L. Cui³, Z. J. Deng³, H. Zhan³,
Y. P. Sun⁴, B. Q. An⁴, J. T. Liang⁵, and Y. S. Chen⁶

¹ CITIC-CBMM Microalloying Technical Center, CITIC Metal Co., Ltd., Beijing 100004, China

hongzhoulu@foxmail.com, guoam@citic.com

² China Automotive Engineering Research Institute Co., Ltd., Chongqing 401122, China
fengyi@caeri.com.cn

³ Maanshan Iron & Steel Company Limited, Maanshan 243003, China

⁴ Yantai Lingyunjiensi Technology Co., Ltd., Yantai 264006, China
{sunyaping, anbaoqin}@lygy.com

⁵ Shougang Research Institute of Technology, Shougang Group Co., Ltd., Beijing 100043, China

⁶ Australian Centre for Microscopy and Microanalysis, The University of Sydney, Sydney, Australia
yi-sheng.chen@sydney.edu.au

Abstract. The press hardening steel (PHS) and hot-stamping components were utilized widely on the reinforcement and lightweight structure of car body due to its ultra-high strength. There existed an obstacle of hydrogen embrittlement (HE) for coated 1.5–2.0 GPa PHS, and uncoated 1.8–2.0 GPa PHS. The typical hot-stamping components were industry-tried by slim Al-Si coated 22MnB5Nb PHS, under -20 °C dew points and without dew point control, and the U-shaped constant bending load test in 0.1 mol/L HCL solution of samples from components were performed based on automotive industry standard T/CSAE155-2020, to compare the hydrogen embrittlement resistance. The results were attained that, under same testing fracture stress, the fracture time is higher obviously for samples at -20 °C dew points comparing to the one without dew point control, and the atmosphere in austenitizing furnace affects prominently the diffusible hydrogen produced by reduction reaction in austenitizing process. A hydrogen embrittlement mechanism deduction is that the original diffusible hydrogen in steel and the diffusible hydrogen produced by reduction reaction in austenitizing process leads to initial micro cracking under higher bending stress according to HELP effect, after that microcrack passivates, and restart of microcrack by the effect of dislocation, grain boundary and applied stress, then hydrogen embrittlement fracture occurs by repeated microcrack passivation and restart.

Keywords: Hydrogen embrittlement · Niobium · Dew point · Austenitizing · Press hardening steel · Hot-stamping components

1 Introduction

Over the last decade, the press hardening steel (short for PHS) and hot-stamping components were utilized widely on the reinforcement and lightweight structure of car body, due to its ultra-high strength. 1.5 GPa-grade tensile strength PHS (e.g. 22MnB5 or 22MnB5-base) has been used for B pillars, A pillars, Bumpers, and Sills etc., by OEMs [1–3], and experienced a rapid growth in the automotive industry [4]. Recently, 1.8–2.0 GPa PHS have also be developed by increasing the carbon content accordingly (0.27–0.37 wt.%C) and controlling various precipitates, thereby attracting great attention as a promising candidate for next-generation reinforcing and lightweight structural components [5–7]. New requirements were presented for such ultra-high strength steel and components, e.g. impact toughness [5], bendability [8], and hydrogen-induced delayed fracture properties [1–4] etc., and hydrogen embrittlement is a severe obstacle and challenge for application of Al-Si coated PHS [9] and 1.8–2.0 GPa PHS [10]. The dew point in the austenitizing furnace can produce hydrogen consequently to the high temperature reaction between water and aluminum/silicon/iron [11], and the high temperature also promotes hydrogen diffusion through the metal lattice under the aluminum-silicon coating, thus increasing the diffusible hydrogen content, after cooling, the coating acts as a strong barrier preventing the hydrogen from going out of the microstructure, this increases the probability of delayed fracture [12]. The atmosphere in austenitizing furnace by dew point control (e.g. -5–40 °C) in new hot stamping lines could reduce the diffusible hydrogen of reduction reaction in austenitizing process, to decrease the hydrogen embrittlement in hot-stamping components [13]. Niobium microalloying has been proved for decreasing hydrogen embrittlement in PHS [1–3, 10, 11]. The coupling of Niobium microalloying and dew point control are considered to decrease the hydrogen embrittlement recently, however, the effect of dew point control on hydrogen embrittlement of Al-Si coated Nb-bearing hot-stamping components should be studied, and the experiments and mechanism study of dew point control for minimizing hydrogen embrittlement in hot-stamping components will be performed in this works.

2 Experimental and Methodology

The 1.4 mm experimental PHS has a chemical composition of Fe-0.23C-0.22Si-1.26Mn-0.17Cr-0.035Nb-0.035V-0.030Ti-0.001B (in weight percent), with a slim Al-Si coating, called as slim AlSi coated 22MnB5Nb. The hot-stamped front door anti-collision beams are industry-trialed using this Nb-bearing PHS, and the steel are heated to 830–950–920 °C in 14 temperature zones of austenitizing furnace during 220 s, and the dew point setting value are at -20 °C and without dew point control respectively. The samples are taken from the hot-stamped components, and the U-shaped constant bending load test of samples are carried out in 0.1mol/L hydrochloric acid solution based on automotive industry standard T/CSAE155–2020 [14], in order to attain the fracture time at various testing stress, and spans are set as 145 mm, 135 mm, 120 mm, 105 mm and 90 mm, two samples are tested in each span. “A” represents the samples with a dew point of -20 °C, “B” represents the samples without dew point control.

3 Results and Discussion

3.1 The Break Time at Various Bending Stress of Samples with Different Dew Point Control

Figure 1(a) and (b) show the results of U-shaped constant bending load test, and no cracking happened for samples with $-20\text{ }^{\circ}\text{C}$ dew point setting value for all 5 spans, but the samples without dew point control cracks at 105 mm and 90 mm spans. The details results could be seen in Table 1 and Table 2.



Fig. 1. The U-shaped constant bending load test results: (a) dew point setting value are at $-20\text{ }^{\circ}\text{C}$; (b) without dew point control.

Table 1. The break time at various bending stress (span) of samples at $-20\text{ }^{\circ}\text{C}$ dew point.

Samples	Span (mm)	Break time (h)	
A-1	145	Not broken in 300 h	
A-2			
A-3			135
A-4			
A-5			
A-6	120		
A-7	105		
A-8			
A-9	90		
A-10			

Table 2. The break time at various bending stress (span) of samples without dew point control.

Samples	Span (mm)	Break time (h)
B-1	145	Not broken in 300 h
B-2		
B-3	135	
B-4		
B-5	120	
B-6		
B-7	105	Broken in 96 h
B-8		
B-9	90	
B-10		

3.2 The Hydrogen Embrittlement Mechanism

Hydrogen embrittlement of lath martensitic steels is characterized by intergranular and “quasi-cleavage” transgranular fracture [15]. Fracture occurs by the synergistic action of the hydrogen-enhanced localized plasticity (short for HELP) [16–20] and decohesion. As a hydrogen trap, dislocations carry hydrogen. When dislocations slip to the grain boundary, most dislocations and the hydrogen carried by them remain in the grain boundary. A large amount of hydrogen in the grain boundary causes the debonding (depolymerization) and hydrogen embrittlement cracking. The intergranular cracking takes place by dislocation pile-ups impinging on prior austenite grain boundaries (short for PAGB) and “quasi-cleavage” is the case when dislocation pile-ups impinge on block boundaries [15]. Crack propagation pass for the hydrogen-related intergranular fracture is PAGB [21–24]. Irrespective of the fracture mode, initiation sites of hydrogen-related cracks are on or in the vicinity of PAGB [25, 26]. PAGB are predominant hydrogen trapping sites in martensite structures [27–29], it can be considered that accumulated hydrogen could induce cracking around PAGB.

However, the hydrogen induced delayed fracture of hot stamping parts is not an instantaneous process, but a continuous and segmented process. From the macro point of view, the parts are cracking continuously, and even the sound of fracture can be heard. From the micro point of view, the microstructure of the crack fracture is stepped [8], which also shows that the cracking is segmented. Passivation involves microcracks here (Fig. 2).

According to HELP, due to the existence of diffusible hydrogen, hydrogen (hydrogen cluster) reduces the activation energy of dislocation slip and promotes the slip of dislocation. As a hydrogen trap, dislocations carry hydrogen. Hydrogen enhances the localized plasticity and microcrack occurs when micro-voids exit, however, passivation occurs at crack tip on loading with or without hydrogen atmosphere, then microcrack propagation pauses. Xie presents a new explanation [30] that low angle GB formed at

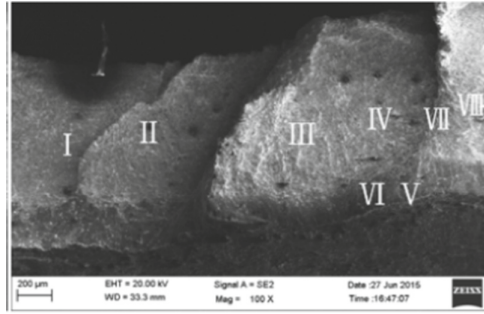


Fig. 2. The Step-Like Morphology microstructure (from I to VIII) of the crack fracture.

crack tip by dislocation emission decorated hydrogen, and passivated crack tip is much more easy to crack again along the low angle GB formed with hydrogen atmosphere.

A hydrogen embrittlement coupling fracture mechanism of hot stamping parts based on HELP mechanism and HEDE mechanism is proposed that, the original diffusible hydrogen in steel and the diffusible hydrogen produced by reduction reaction in austenitizing process leads to initial micro cracking under higher bending stress according to HELP effect, after that microcrack tip passivates, and restart of microcrack caused by dynamic formation of GBs by dislocation emission and applied stress, the microcrack propagates by repeated microcrack tip passivation and reboot. When the crack impinges on PAGB or block boundaries, then hydrogen embrittlement fracture occurs, because GBs in hydrogen atmosphere have much stronger HEDE effect.

In this paper, the reduction hydrogen generation reaction is partially inhibited by $-20\text{ }^{\circ}\text{C}$ dew point control, the diffusible hydrogen in A sample is less than that in B sample, then the slip of dislocation and initial micro cracking are less for A samples. For B samples, more diffusible hydrogen promotes the slip of dislocation and initial micro cracking, when the higher stress applied (e.g., 105 mm and 90 mm spans), the microcrack propagates by repeated microcrack tip passivation and reboot, the samples cracks.

The stress corresponding to 105 mm and 90 mm spans are 1542 and 1574 MPa respectively, while the stress corresponding to 120 mm span is 1484 MPa. Table 2 shows that slim AlSi coated 22MnB5Nb PHS doesn't crack under the process conditions without dew point control and under the applied load conditions close to the material tensile strength (1484 MPa \approx 0.9 times the tensile strength). Under $-20\text{ }^{\circ}\text{C}$ dew point process condition, slim 22MnB5Nb PHS doesn't crack under all applied load conditions, and its hydrogen embrittlement resistance was further improved.

4 Conclusions

Using U-shaped constant bending load test of samples from components by slim Al-Si coated 22MnB5Nb PHS, no cracking for all samples under $-20\text{ }^{\circ}\text{C}$ dew points and 1574 MPa stress in 300 h in 0.1 mol/L HCL solution immersion. No cracking for samples without dew point control under the applied load conditions close to the material tensile

strength (1484 MPa \approx 0.9 times the tensile strength, 120 mm span), but the samples without dew point control cracks with higher stress applied (\geq 1542 MPa stress, e.g., 105 mm and 90 mm spans) in 96 h. The reduction hydrogen generation reaction is partially inhibited by -20 °C dew point control, and the higher applied stress promotes reboot of microcrack tip passivation and the microcrack propagates.

Acknowledgments. This work is supported by Grant No. 2021FWNB30047 of the CITIC-CBMM Nb Steel Award Fund Program. Work partially supported by grant No. Grant No. LP180100431 of Linkage Projects of Australian Research Council.

References

1. H. Z. Lu, S. Q. Zhang, B. Jian, H. Mohrbacher and A. M. Guo, Solutions for Hydrogen-Induced Delayed Fracture in Hot Stamping, *Advanced Materials Research* **1063**, 32 (2014).
2. B. Jian, W. Li, H. Mohrbacher, H. Z. Lu and W. J. Wang, Development of niobium alloyed press hardening steel with improved properties for crash performance, *Advanced Materials Research* **1063**, 7 (2015).
3. S. Zhang, Y. Huang, B. Sun, Q. Liao, H. Lu, B. Jian, H. Mohrbacher, W. Zhang, A. Guo and Y. Zhang, Effect of Nb on hydrogen-induced delayed fracture in high strength hot stamping steels, *Materials Science & Engineering A* **626**, 136 (2015).
4. *The state-of-art study in global car body and automotive lightweight technology*. (Beijing Institute of Technology Press, 2019).
5. J. Wang, Y. Liu, Q. Lu, J. Pang and C. D. Horvath, Effect of microstructure on impact toughness of press-hardening steels with tensile strength above 1.8 GPa, *Iron and Steel Technology* **14**, 104 (2017).
6. J. Liang, Z. Zhao, B. Sun, H. Z. Lu, J. H. Liang, Q. He and W. J. Chen, A novel ultra-strong hot stamping steel treated by quenching and partitioning process, *Materials Science and Technology* **34**, 2241 (2018).
7. J. Bian, H. Z. Lu, W. J. Wang and A. M. Guo, Alloying design and process strategy for high performance 1800 MPa press hardening steel, in *4th International Conference on Advanced High Strength Steel and Press Hardening*, (Hefei, China, 2018).
8. M. T. Ma, Y. Zhao, H. Z. Lu, J. Bian, A. M. Guo and Z. F. Sun, The Cold Bending Cracking Analysis of Hot Stamping Door Bumper, in *The International Conference on Advanced High Strength Steel and Press Hardening*, (Xian, China, 2016).
9. L. Cho, D. H. Sulistiyo, E. J. Seo, R. J. Kyoung, W. K. Seng, K. O. Jim, Y. R. Cho and B. C. De Cooman, Hydrogen absorption and embrittlement of ultra-high strength aluminized press hardening steel, *Materials Science and Engineering* **734**, 416 (2018).
10. M. C. Jo, J. Yoo, S. Kim, S. Kim, J. K. Oh, J. Bian, S. S. Sohn and S. Lee, Effects of Nb and Mo alloying on resistance to hydrogen embrittlement in 1.9 GPa-grade hot-stamping steels, *Materials Science and Engineering: A* **789**, 139656, (2020).
11. H. Z. Lu, J. Bian, A. M. Guo and Y. S. Chen, The effect and mechanism of niobium for decreasing hydrogen embrittlement in hot-stamping components, in *Advanced High Strength Steel and Press Hardening, the proceeding of the 5th International conference* (Shanghai, China, 2020).
12. A. Cherubini, L. Bacchi, S. Corsinovi, M. Beghini and R. Valentini, Hydrogen embrittlement in advanced high strength steels and ultra-high strength steels: a new investigation approach, *Procedia Structural Integrity* **13**, 753 (2018).

13. B. Dvorak, J. J. Tawk and T. Vit, Advanced design of continuous furnace for hot stamping line, in *The 2nd International Conference on Advanced High Strength Steel and Press Hardening* (Changsha, China, 2015).
14. Specification for Testing and Evaluation of Susceptibility to Hydrogen-induced Delayed Fracture of Ultra-high: T/CSAE155-2020 (2020).
15. A. Nagao, M. Dadfarnia, B. P. Somerday, P. Sofronis and R. O. Ritchie, Hydrogen-enhanced-plasticity mediated decohesion for hydrogen-induced intergranular and ‘quasi-cleavage’ fracture of lath martensitic steels, *Journal of the Mechanics and Physics of Solids* **112**, 403 (2018).
16. C. D. Beachem, A new model for hydrogen-assisted cracking (hydrogen “embrittlement”), *Metallurgical and Materials Transactions B* **3**, 441 (1972).
17. H. K. Birnbaum and P. Sofronis, Hydrogen-enhanced localized plasticity—a mechanism for hydrogen-related fracture, *Materials Science & Engineering A* **176**, 191 (1994).
18. S. P. Lynch, Environmentally assisted cracking: overview of evidence for an adsorption-induced localized-slip process, *Acta Metallurgical* **36**, 2639 (1988).
19. P. J. Ferreira, I. M. Robertson and H. K. Birnbaum, Hydrogen effects on the interaction between dislocations, *Acta Materialia* **46**, 1749 (1998).
20. I. M. Robertson, P. Sofronis, A. Nagao, M. L. Martin, S. Wang, D. W. Gross and K. E. Nygren, Hydrogen embrittlement understood, *Metallurgical & Materials Transactions A* **46**, 1085 (2015).
21. S. K. Banerji, C. J. McMahon and H. C. Feng, Intergranular fracture in 4340-type steels: effects of impurities and hydrogen, *Metallurgical Transactions A* **9**, 237 (1978).
22. D. C. Bruce and K. George, The structure of tempered martensite and its susceptibility to hydrogen stress cracking, *Metallurgical Transactions A* **11**, 1799 (1980).
23. M. Wang, E. Akiyama and K. Tsuzaki, Effect of hydrogen and stress concentration on the notch tensile strength of AISI 4135 steel, *Materials Science & Engineering A* **398**, 37 (2005).
24. A. Shibata, T. Matsuoka, A. Ueno and N. Tsuji, Fracture surface topography analysis of the hydrogen-related fracture propagation process in martensitic steel, *International Journal of Fracture* **205**, 73 (2017).
25. A. Shibata, T. Murata, H. Takahashi, T. Matsuoka and N. Tsuji, Characterization of hydrogen-related fracture behavior in as-quenched low-carbon martensitic steel and tempered medium-carbon martensitic steel, *Metallurgical and Materials Transactions A* **46**, 5685 (2015).
26. A. Shibata, Y. Momotani, T. Murata, T. Matsuoka, M. Tsuboi and N. Tsuji, Microstructural and crystallographic features of hydrogen-related fracture in lath martensitic steels, *Materials Science & Technology* **33**, 1524 (2017).
27. José Ovejero-García, Hydrogen microprint technique in the study of hydrogen in steels, *Journal of Materials Science* **20**, 2623 (1985).
28. K. Takai, J. Seki and Y. Homma, Observation of trapping sites of hydrogen and deuterium in high-strength steels by using secondary ion mass spectrometry, *Materials Transactions* **36**, 1134 (1995).
29. Y. Momotani, A. Shibata, D. Terada and N. Tsuji, Effect of strain rate on hydrogen embrittlement in low-carbon martensitic steel, *International Journal of Hydrogen Energy* **42**, 3371 (2017).
30. D. G. Xie, L. Wan and Z. W. Shan, Hydrogen enhanced cracking via dynamic formation of grain boundary inside aluminium crystal, *Corrosion Science* **183**, 109307 (2021).

Open Access This chapter is licensed under the terms of the Creative Commons Attribution-NonCommercial 4.0 International License (<http://creativecommons.org/licenses/by-nc/4.0/>), which permits any noncommercial use, sharing, adaptation, distribution and reproduction in any medium or format, as long as you give appropriate credit to the original author(s) and the source, provide a link to the Creative Commons license and indicate if changes were made.

The images or other third party material in this chapter are included in the chapter's Creative Commons license, unless indicated otherwise in a credit line to the material. If material is not included in the chapter's Creative Commons license and your intended use is not permitted by statutory regulation or exceeds the permitted use, you will need to obtain permission directly from the copyright holder.

